

---

## Mirror Alignment and Optical Quality of the H.E.S.S. Imaging Atmospheric Cherenkov Telescopes

---

René Cornils and Götz Heinzelmann

*Universität Hamburg, Institut für Experimentalphysik, Luruper Chaussee 149, D-22761 Hamburg, Germany*

Stefan Gillessen, Ira Jung, and Werner Hofmann

*Max-Planck-Institut für Kernphysik, P.O. Box 103980, D-69029 Heidelberg, Germany*

---

### Abstract

The alignment of the mirror facets of the H.E.S.S. imaging atmospheric Cherenkov telescopes is performed by a fully automated alignment system using stars imaged onto the lid of the PMT camera. In order to be adjustable, the mirror facets are mounted onto supports which are equipped with two motor-driven actuators while optical feedback is provided by a CCD camera viewing the lid. The alignment procedure, implying the automatic analysis of CCD images and control of the mirror alignment actuators, has been proven to work reliably. On-axis, 80% of the reflected light is contained in a circle of less than 1 mrad diameter, well below specifications.

### 1. Introduction

H.E.S.S. (Hofmann 2002) is a stereoscopic system of large imaging atmospheric Cherenkov telescopes currently under construction in the Khomas Highland of Namibia with the first telescope already in operation. The reflector of each telescope consists of 380 mirror facets with 60 cm diameter and a total area of 107 m<sup>2</sup>. For optimum imaging qualities, the alignment of the mirror facets is crucial. A fully automated alignment system has been developed, including motorized mirror supports, compact dedicated control electronics, various algorithms and software tools. The specification for the performance of the complete reflector requires the resulting point spread function to be well below the size of a pixel of the Cherenkov camera with a rms projected angle of about 0.7 mrad. The resulting rms width of the point spread function should thus not exceed 0.5 mrad.

## 2. Adjustable mirror support

A mirror unit consists of a support triangle carrying one fixed mirror support point and two motor-driven actuators. A motor unit includes the drive motor, two Hall sensors shifted by  $90^\circ$  sensing the motor revolutions and providing four TTL signals per turn, and a 55:1 worm gear. The motor is directly coupled to a 12mm threaded bolt, driving the actuator shaft by 0.75mm per revolution. One count of the Hall sensor corresponds to a step size of  $3.4\text{ }\mu\text{m}$ , or 0.013mrad tilt of the mirror. The total range of an actuator is about 28mm.

## 3. Mirror alignment technique

The alignment uses the image of an appropriate star on the closed lid of the PMT camera, viewed with a CCD camera at the center of the dish as illustrated in Fig. 1. (left) (see Cornils & Jung (2001) and references therein). The individual mirrors are adjusted with the goal to combine the star images by all mirrors into a single spot at the center of the PMT camera. The basic

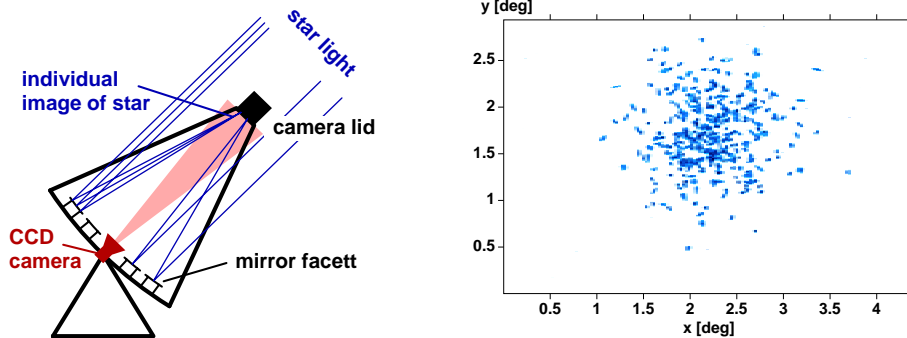


**Fig. 1.** *Left:* Mirror alignment technique. The telescope is pointed towards an appropriate star whereupon all mirror facets generate individual images of the alignment star in the focal plane. Actuator movements change the location of the corresponding light spot. This is observed by a CCD camera viewing the lid of the PMT camera which acts as the screen. *Right:* Image of a star on the camera lid before alignment (log. intensity scale). Each spot corresponds to a mirror facet.

algorithm is as follows: a CCD image of the camera lid is taken. At the start of the alignment, with all actuators positioned roughly at the center of their range, this image might look like Fig. 1. (right). The two actuators of the mirror which is to be aligned are then moved one by one, changing the location of the corresponding spot. These displacements are recorded by the CCD camera and provide all information required to subsequently position the spot at the center

of the main focus. This procedure is repeated for all mirrors in sequence.

It is – to our knowledge – the first time that such a technique is used to align the mirrors of Cherenkov telescopes. The major advantages of this approach are evident: a natural point-like source at infinite distance is used and the alignment can be performed at the optimum elevation ( $55^\circ$ – $75^\circ$  in the case of H.E.S.S.).

### 3.1. Alignment algorithm and procedure

To study the quality of different alignment algorithms, a tool has been developed simulating the complete mirror support (not including mechanical play). Due to the uncertainty of one Hall count in each actuator, the theoretical optimum is characterized by a projected deviation for individual light spots in the focal plane of 0.011 mrad rms. After simulating the alignment accuracy for various different approaches, a robust algorithm was chosen whose projected deviation of 0.017 mrad rms is still small compared to the average intrinsic point spread function of the mirror facets of 0.176 mrad. In addition to achieving a high alignment accuracy, the algorithm should allow a fast and reliable realignment of the mirror facets in case the point spread function is observed to deteriorate over time. This was accomplished by splitting the procedure into two parts. During the *initial alignment*, all relevant values, i.e. the range and position of the actuators and the matrix to transform between CCD and actuator coordinates, are determined and stored into a database for further usage. The *realignment* procedure does not redetermine these values but simply retrieves them from the database.

Under normal circumstances, the initial alignment needs about two weeks and the realignment can be performed in one to two nights. The steps requiring optical feedback can be performed while the moon is partially visible, thus not interfering with normal data taking.

## 4. Point spread function

To study the point spread function after the mirror alignment of the first telescope was completed (Fig.2., left), a variety of stars were used, covering a wide range of locations within the field of view and of elevation and azimuth angles of the telescope pointing. Fig. 2. (right) shows a CCD image of the image of a star on the camera lid in relation to the size of a hexagonal PMT pixel. The intensity distribution is symmetrical without pronounced substructure and the width of the spot is well below the PMT pixel size.

To parameterize the width of the intensity distributions, different quantities are used, in particular the rms width  $\sigma_{proj}$  of the projected (1-dimensional) distributions and the radius  $r_{80\%}$  of a circle around the center of gravity of the

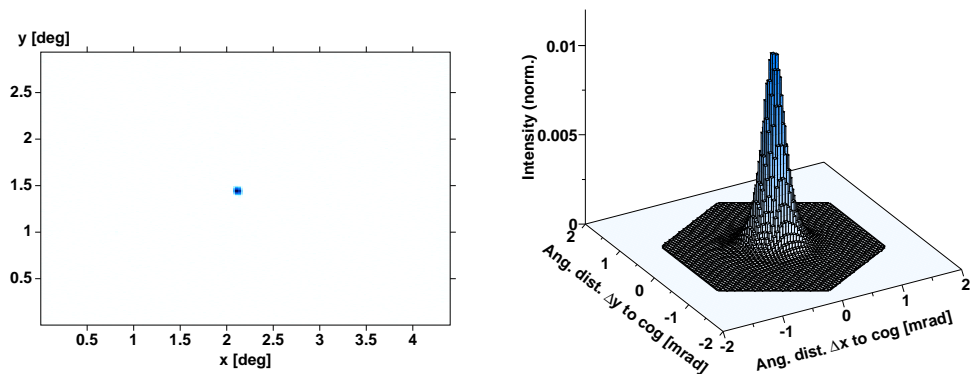


**Fig. 2.** *Left:* Image of a star on the camera lid after the alignment of all mirrors (log. intensity scale). *Right:* The corresponding intensity distribution. The hexagonal border indicates the size of a pixel of the PMT camera.

image, containing 80% of the total intensity. On the optical axis, the point spread function achieved is characterized by the values  $\sigma_{proj} = 0.24$  mrad and  $r_{80\%} = 0.42$  mrad, well below specifications (0.5 and 0.9 mrad, respectively).

#### 4.1. Variation of the point spread function across the field of view

Optical aberrations are significant in Cherenkov telescopes due to their single-mirror design and the small  $f/d$  ratios. At some distance from the optical axis, one therefore expects the width of the point spread function to grow linearly with the angle  $\theta$  to the optical axis. With increasing inclination to the optical axis the spot is indeed observed to widen. For elevation angles around  $65^\circ$  where the mirrors were aligned, Fig. 3. (left) summarizes the spot parameters as a function of the angle  $\theta$  to the optical axis. Besides  $r_{80\%}$ , the rms widths on the distributions projected on the radial ( $\sigma_{radial}$ ) and tangential ( $\sigma_{tangential}$ ) directions are given. The radial axis goes from the camera center to the center of the spot, the tangential axis is the corresponding orthogonal direction. The measurements demonstrate that the spot width depends primarily on  $\theta$ ; no other systematic trend has been found.

To verify that the measured intensity distribution is quantitatively understood, Monte Carlo simulations of the actual optical system were performed, including the exact locations of all mirrors, shadowing by camera masts, etc. As further input, the measured average spot size of 0.176 mrad for the mirror facets and the simulated precision of the alignment algorithm were used; the latter contribution is virtually negligible. The results are in excellent agreement with the measurements.

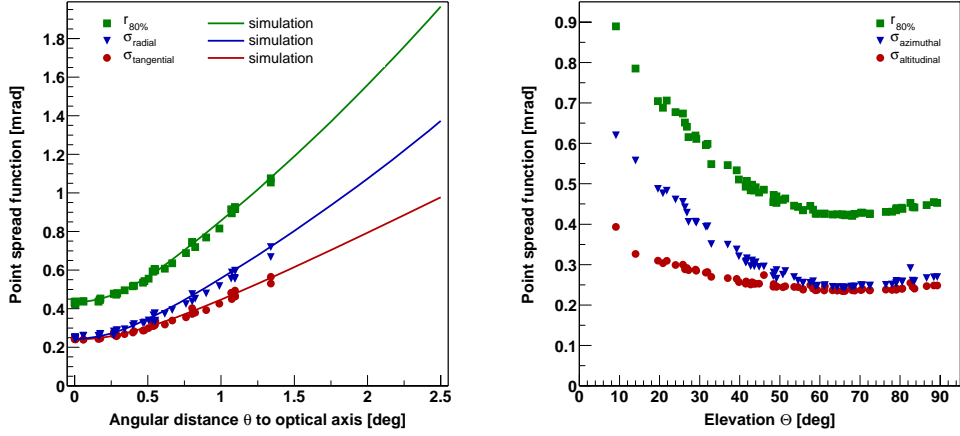


**Fig. 3.** *Left:* Width of the point spread function as a function of the angular distance  $\theta$  to the optical axis at elevations around  $65^\circ$ . *Right:* Width of the point spread function as a function of telescope elevation  $\Theta$ .

#### 4.2. Variation of the point spread function with telescope pointing

At fixed elevation, no significant dependence of the point spread function on telescope azimuth was observed. In contrast, a variation with elevation is expected due to gravity-induced deformations of the telescope structure. Fig 3. (right) illustrates how the spot width changes with elevation. The width can be approximated by a flat parabola with its minimum around  $65^\circ$ , the mean alignment elevation. For elevation angles most relevant for Cherenkov observations, i.e. above  $45^\circ$ , the spot size  $r_{80\%}$  varies by less than 10%. At  $30^\circ$  it is about 40% larger than the minimum size but still well below the size of the PMT pixels.

### 5. Deformation of the dish structure

From the behaviour of the point spread function alone, it is hard to deduce what kind of deformations are responsible for the widening of the spot with varying elevation. But the alignment system implements a feature which allows to study the deformation of the support structure in detail. Rather than combining all individual spots to a uniform main spot, the spots can be arranged in arbitrary patterns. Fig. 4. (left) shows the spots corresponding to individual mirror facets arranged in the form of a square matrix; each element of the matrix is the image generated by one mirror. By taking CCD images of the matrix at different elevations, the relative movement of individual spots indicates the deflection of the corresponding mirror facets due to the deformation of the support structure at the location of the mirrors. As an example, Fig. 4. (right) shows the deflec-

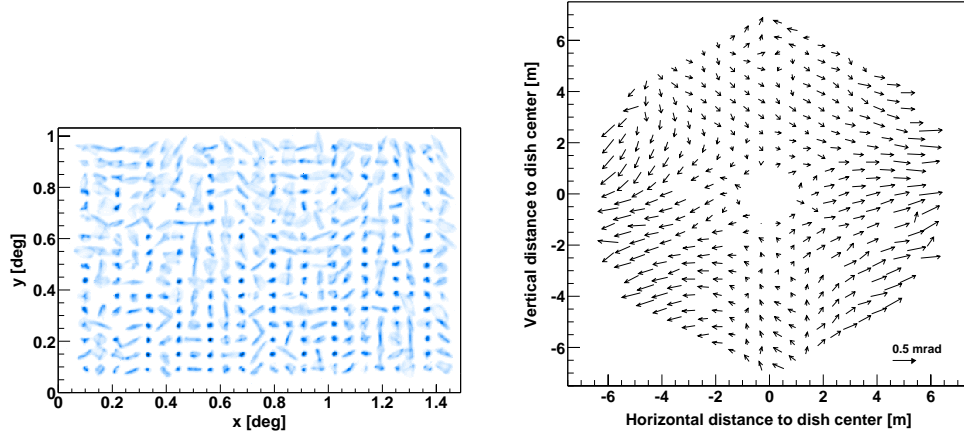


**Fig. 4.** *Left:* Individual spots arranged in the form of a matrix. Each spot corresponds to the image of the observed star generated by a single mirror facet. *Right:* Mirror deflections at  $29^\circ$  elevation with respect to  $65^\circ$ ; arrows scaled by  $\sqrt{\text{deflection}}$ .

tion of the mirror facets at  $29^\circ$  elevation with respect to  $65^\circ$ , the mean alignment elevation. It can be seen that deformations are particularly strong at the outer edges where the camera arms are attached.

## 6. Conclusion

The mirror alignment of the first H.E.S.S. telescope was a proof of concept and a test of all technologies involved: mechanics, electronics, software, algorithms and the alignment technique itself. All components work as expected and the resulting point spread function exceeds the specifications by a significant margin. The widening of the spot with increasing angle to the telescope axis is in accordance with the expected behaviour based on simulations and the variation of spot size with elevation due to deformations of the support structure is completely uncritical for the whole working range.

## References

1. Bernlöhner K., Carrol O., Cornils R., Elfahem S. et al. 2002, The optical system of the H.E.S.S. imaging atmospheric Cherenkov telescopes, Part I, in prep.
2. Cornils R., Gillessen S., Jung I., Hofmann W. et al. 2002, The optical system of the H.E.S.S. imaging atmospheric Cherenkov telescopes, Part II, in prep.
3. Cornils R., Jung I. 2001, Proc. of the Int. Cosmic Ray Conf., vol. 7, 2879
4. Hofmann W. 2002, these proceedings